

BamA β 16C strand and periplasmic turns are critical for outer membrane protein insertion and assembly

Yinghong Gu^{1,*}, Yi Zeng^{1,*}, Zhongshan Wang^{1,2,3,*} and Changjiang Dong¹

¹Biomedical Research Centre, Norwich Medical School, University of East Anglia, Norwich Research Park, Norwich, NR4 7TJ, UK;

²Jiangsu Province Key Laboratory of Anesthesiology, Xuzhou Medical University, Xuzhou 221004, China;

³Key Laboratory of Bio-resources and Eco-environment, Ministry of Education, Sichuan Key Laboratory of Molecular Biology and Biotechnology, College of Life Sciences, Sichuan University, Chengdu, 610064, China.

Correspondence: Changjiang Dong (C.Dong@uea.ac.uk)

*These authors contributed equally to this work.

Abstract

Outer membrane β -barrel proteins play important roles in importing nutrients, exporting wastes and conducting signals in Gram-negative bacteria, mitochondria and chloroplasts. The outer membrane proteins are inserted and assembled into the outer membrane by OMP85 family proteins. In *Escherichia coli*, the β -barrel assembly machinery (BAM) contains four lipoproteins BamB, BamC, BamD and BamE, and one outer membrane protein BamA, forming a “top hat”-like structure. Structural and functional studies of the *E. coli* BAM machinery have revealed that the rotation of periplasmic ring may trigger the barrel β 1C- β 6C scissor-like movement that promote the unfolded outer membrane protein insertion without using ATP. Here we report the BamA C-terminal barrel structure of *Salmonella enterica* Typhimurium str. LT2 and functional assays, which reveal that the BamA’s C-terminal residue Trp, the β 16C strand of the barrel and the periplasmic turns are critical for the functionality of BamA. These findings indicate that the unique β 16C and the periplasmic turns of BamA are important for the out membrane insertion and assembly. The periplasmic turns might mediate the rotation of the periplasmic ring to the scissor-like movement of BamA β 1C- β 6C, triggering the outer membrane protein insertion. These results are important for understanding the outer membrane protein insertion in Gram-negative bacteria, as well as in mitochondria and chloroplasts.

Introduction

Outer membrane proteins (OMPs) play important roles in importing nutrients, exporting wastes and transporting biological molecules in Gram-negative bacteria, mitochondria and chloroplasts [1, 2]. Mitochondria and chloroplasts are eukaryotic organelles that derived from bacterial endosymbionts of α -proteobacteria and cyanobacteria [2], respectively. The OMPs are inserted and assembled into the outer membrane (OM) by conserved OMP85 family proteins, which share the C-terminal 16 β -stranded barrel structure with different numbers of N-terminal polypeptide transport associated (POTRA) domains [3-10]. In Gram-negative bacteria, BamA is the main OMP85 family protein for outer membrane insertion, while OMP85 family proteins SAM50 and OEP80 are proposed to be responsible for outer membrane protein insertion in mitochondria and chloroplasts [7-10], respectively, suggesting that the SAM50 and OEP80 may use a similar mechanism as BamA to insert outer membrane proteins.

In *E. coli*, the unfolded OMPs are synthesized in the cytoplasm, and transported across the inner membrane (IM) by SecYEG complex to the periplasm, where the unfolded OMPs are escorted by chaperon proteins Skp and SurA to the beta-barrel assembly machinery (BAM) complex for insertion [11]. The *E. coli* BAM machinery complex contains an OMP BamA and four lipoproteins BamB, BamC, BamD and BamE, of which BamA and BamD are essential [12]. Individual crystal structures of BamA, BamB, BamC, BamD and BamE have been determined, as well as structures of two protein complexes BamCD, BamB with POTRA3 and 4, and BamD with POTRA4 and 5 [7, 13-28]. In addition, The OEP80 of chloroplasts is evolutionally from cyanobacteria Omp85 proteins, which are structurally characterized with three POTRA domains with a unique loop at POTRA domain 3. The loop is reported to

regulate the barrel pore [3, 4]. More recently, crystal structures of four-protein subcomplex BamACDE [29, 30] and five-protein full complex BamABCDE [29, 31] with functional assays and molecular dynamics simulations have been reported, as well as the cryo-EM structure of the BAM complex [32]; these revealed that the five POTRA domains of BamA and the BamB, BamC, BamD and BamE form a ring architecture in the periplasm and the rotation of the ring structure may promote the scissor-like movement of the β 1C- β 6C of BamA barrel for OMP insertion [29]. The crystal structures showed that the BAM complex in two distinct conformations and functional assays have confirmed that the two states exist in *E. coli* [29]. In the BamABCDE complex, the β 16C of BamA barrel coils into the lumen; however, whether the shift of the β 16C is critical and how the rotation of the ring structure promotes the scissor-like movement are unknown. In contrast to *E. coli* BAM complex, it has been reported that the *Salmonella* BamB can play a role independent of BAM machinery and BamD is not essential for *Salmonella* [33], suggesting that the BAM machinery subunits may be different from those of *E. coli*. Here, we report the crystal structure of BamA from *S. enterica*, which shows that the β 16C partially coils into the barrel. We then show the importance of the last residue (tryptophan). Finally, we demonstrate that the periplasmic turns are essential, possibly involved in mediating the periplasmic ring rotation to the β 1C- β 6C scissor-like movement, while the extracellular loops 1-3 play less important role for OMP insertion.

Materials and Methods

Plasmid construction

Primers used in this study are listed in Table S1. The *bamA* and *bamB* genes were amplified by polymerase chain reaction (PCR) from genomic DNA of *Salmonella*

Typhimurium str. LT2. The *bamB* was cloned into pACYCDuet-1 (Novagen) between *Nco* I and *Hind* III sites, and the *bamA* was sequentially cloned into *Nde* I and *Xho* I sites. A hexahistidine (His₆) tag was introduced into BamA between Gly23 and Phe24 using site-directed mutagenesis [34], resulted in expression construct pACYC-SenBamAB. The nucleotide sequences were verified by Sanger sequencing. Plasmid pYG91 containing *pelB*-His₁₀-EcoBamA was constructed previously [29] for *E. coli* BamA functional assays.

Protein expression and purification

The recombinant plasmid pACYC-SenBamAB was transformed into *E. coli* BL21(DE3) cells (Novagen) for overexpression. An overnight culture was inoculated in Miller's LB Broth medium supplemented with 34 $\mu\text{g ml}^{-1}$ chloramphenicol and the cells were grown at 37°C to $A_{600\text{ nm}}$ of 0.3-0.4, and then shifted to 25°C. When $A_{600\text{ nm}}$ reached 0.5-0.7, expression of SenBamAB was induced with isopropyl β -D-thiogalactopyranoside (IPTG) at a final concentration of 100 $\mu\text{mol l}^{-1}$ at 20°C overnight. Twelve litres of the cells were harvested by centrifugation and resuspended in lysis buffer [20 mM Tris-HCl (pH 8.0), 150 mM NaCl, 5 $\mu\text{g ml}^{-1}$ DNase I and 100 $\mu\text{g ml}^{-1}$ lysozyme], and then disrupted at 30,000 p.s.i. using a cell disruptor (Constant Systems Ltd). Cell debris and unbroken cells were removed by centrifugation and the resulting supernatant was ultracentrifuged at 100,000 g for 1 h at 4°C. The membrane fraction was resuspended in 20 mM Tris-HCl (pH 8.0) and 150 mM NaCl supplemented with 1% (w/v) N-lauroylsarcosine sodium salt (Sigma-Aldrich) and incubated for 1 h at room temperature with moderate rocking, and then ultracentrifuged again. The pellet was resuspended in solubilization buffer [20 mM Tris-HCl (pH 8.0), 300 mM NaCl, 10 mM imidazole and 1% SB3-14 (Sigma-Aldrich)]

and solubilized overnight at 4°C with moderate rocking. The solubilized membrane was ultracentrifuged and the resulting supernatant was applied to a pre-equilibrated Ni-NTA superflow resin column (Qiagen). The His-tagged proteins were eluted with elution buffer [20 mM Tris-HCl (pH 8.0), 300 mM NaCl, 300 mM imidazole, 0.023% (w/v) n-Dodecyl-N,N-Dimethylamine-N-Oxide (LDAO; Anatrace) and 0.53% (w/v) n-Octyl-β-D-Glucopyranoside (OG; Anatrace)] after wash the resin with 20 column volumes of wash buffer [20 mM Tris-HCl (pH 8.0), 300 mM NaCl, 30 mM imidazole, 0.023% (w/v) LDAO and 0.53% (w/v) OG]. The eluent was further purified by size-exclusion chromatography (HiLoad 16/600 Superdex 200 prep grade column; GE Healthcare) in gel filtration buffer [20 mM Tris-HCl (pH 7.8), 100 mM NaCl, 0.023% (w/v) LDAO and 0.53% (w/v) OG]. Fractions containing SenBamAB were pooled and concentrated to 6 mg ml⁻¹ for crystallization.

Crystallization, data collection and structure determination

The purified SenBamAB complex was crystallized using a sitting-drop vapour diffusion method at 22°C. Crystal trials were set up using various commercial crystallization screen conditions. A drop of reservoir solution (0.15 or 0.3 μl) was mixed with an equal amount of protein solution using a crystallization robot Gryphon (Art Robbins Instruments). Crystals were obtained in a buffer containing 0.1 M HEPES sodium (pH 7.5) and 1.0 M sodium citrate tribasic dehydrate. Crystals were harvested and cryoprotected in 20% glycerol supplemented with the precipitation solution, and then flash-cooled and stored in liquid nitrogen. X-ray diffraction data were collected at Diamond Light Source (UK) on beamline I04-1 at a wavelength of 0.9200Å, and indexed by iMosflm and further processed with CCP4 package [35]. Data collection and refinement statistics are summarised in Table 1. The structure

was solved by molecular replacement method with Phaser [36] in CCP4 suite [35] using an *E. coli* BamA beta-barrel structure (Protein Data Bank accession code: 4N75) as the search model. The structure was built in Coot [37] and structure was refined using REFMAC5 [38]. The final model was validated with $R_{\text{work}}/R_{\text{free}}$ values of 0.28/0.34 (Table 1).

Site-directed mutagenesis

Primers used for site-directed mutagenesis of *E. coli* BamA are listed in Table S1. A pRSFDuet-1 based construct, pYG91, containing coding sequences of an N-terminal pelB signal peptide followed by a decahistidine (His₁₀) tag and the mature peptide of *E. coli* BamA starts from Glu22, was used as template for PCR [29]. Site-directed mutagenesis was performed according to the protocol of Liu and Naismith [34], with minor modifications. All mutants were confirmed by Sanger sequencing.

Plate complementation assays

E. coli JCM166 cells [5], a BamA depletion strain, were used for functional assays. Plasmid pRSFDuet-1 (empty vector control), pYG91 (wild type BamA) or BamA mutants were transformed into JCM166 competent cells, respectively. Single colony from LB agar plate containing 50 $\mu\text{g ml}^{-1}$ kanamycin, 100 $\mu\text{g ml}^{-1}$ carbenicillin and 0.05% L-(+)-arabinose was inoculated in 10 ml LB medium supplemented with antibiotics and L-(+)-arabinose, and cultured overnight at 37°C. The cells were collected by centrifugation, and resuspended in fresh LB medium. After another centrifugation, the cell pellet was resuspended and diluted to $A_{600\text{ nm}}$ of ~0.3. And then, the cells were streaked onto LB agar plates supplemented with antibiotics and incubated overnight at 37°C.

Western blotting

To assess the expression levels of BamA in cell membrane, recombinant cells were cultured in 50 ml LB medium supplemented with antibiotics and L-(+)-arabinose for overnight at 37°C. The cells were pelleted, resuspended in Tris-buffered saline [TBS, 20 mM Tris-HCl (pH 8.0) and 150 mM NaCl] and lysed by sonication. The lysate was clarified by centrifugation and the resultant supernatant was ultracentrifuged. The cell membrane was resuspended and solubilized in TBS supplemented with 1% SB3-14 for 30 min at room temperature. Membrane protein samples were mixed with 5 × SDS–PAGE loading buffer and boiled. Proteins were resolved by SDS-PAGE on a 4-12% gradient gel (Invitrogen) and transferred onto a PVDF membrane. The membrane was blocked overnight in Pierce™ Protein-Free (TBS) Blocking Buffer (Thermo Fisher Scientific) and then incubated with His-Tag Monoclonal Antibody (1:1,000, Millipore) or anti-*E. coli* OmpA polyclonal antibody (Antibody Research Corporation). IRDye 800CW goat anti-mouse IgG (H+L) or IRDye 800CW donkey anti-rabbit IgG (H+L) (1:5,000, LI-COR Biosciences) was used as secondary antibody. The blot was scanned using the 800 nm channel of the Odyssey Infrared Imaging System (LI-COR Biosciences).

Urea extraction assays

To determine BamA insertion, urea extraction assays were performed [39]. Briefly, cell pellets were resuspended in 10 mM HEPES and sonicated, the un-lysed cells and cell debris were removed and the cell membrane was isolated. The inner membrane was solubilized with 2% (w/v) N-lauroyl sarcosine solution, the outer membrane was isolated by ultracentrifugation and resuspended in urea-containing (6

M urea) extraction solution. After incubation and ultracentrifugation, the pelleted membrane fractions were collected and resuspended in MilliQ water. Samples were analysed by SDS-PAGE and Western blotting.

Heat modifiability assays

BamA mutant was transformed into JCM166 cell and cultured in LB medium supplemented with antibiotics and L-(+)-arabinose. Cell membrane was isolated and solubilized, and the boiled or un-boiled membrane protein samples were resolved by SDS-PAGE at 4°C. The proteins were transferred from the gel to PVDF membrane and western blotting was performed as described above.

Results

BamA Structure of *S. enterica*

The BamA and BamB of *S. enterica* were co-expressed, and the BamAB complex was purified (Figure 1 A, Figure S1). Crystallization trials of BamAB complex were performed. The crystals belong to space group P6₂22 with cell dimensions $a = b = 124.03\text{\AA}$, $c = 131.48\text{\AA}$, $\alpha = \beta = \gamma = 90^\circ$. The crystal structure was determined by molecular replacement to a resolution of 2.92 Å. Only the BamA barrel domain was found in the structure, indicating that the BamAB complex may be too flexible to be crystallized, while the BamA POTRA domains and BamB may be cleaved by contaminant proteases during the protein crystallization. There is one BamA molecule per asymmetric unit. The BamA barrel is formed by 16 β -strands with residues Asn427-Gly801 (Figure 1B, Figure S2). Secondary-structure matching (SSM) analysis revealed that the BamA structure of *S. enterica* is very similar to those of the *E. coli* (PDB code 5D0O) with a root-mean-square deviation (RMSD) of

1.85 Å over 379 Ca atoms [40]. The obvious differences between the two barrel structures are that the extracellular loops 4 and 6 of *S. enterica* are shorter than those of the *E. coli* by 4 and 3 residues, respectively (Figure 1A, Figure S2). It is worth noting that the β 16C of *S. enterica* BamA is very similar to those of the *E. coli* BamA of BamABCDE (Figure 1C), in which the β 16C coils into the barrel, while β 16C of *E. coli* BamA of BamACDE is further rotated into the barrel (Figure S3). The significant conformational changes of the periplasm turns are observed with T1, T2 and T6 in particular (Figure S4).

Trp810 of the BamA C-terminal residue is important for BamA insertion

It is reported that the last β -strand of bacterial outer membrane barrel containing a β -signature sequence, which contains Phe (Trp) at the C-terminus and hydrophobic residues at positions 3, 5, 7 and 9 from the C-terminus [41]. This motif is conserved in Gram-negative bacteria outer membrane β -barrel proteins with the particular important C-terminal residue Phe (Trp). However, a recent study suggest that the *E. coli* BamA's β -signature sequence is residues N765-P779, which forms the strand β 14C rather than the last strand β 16C [42]. For functional assays, we use the *E. coli* BamA depletion strain JCM166 and the plasmid pYG91 containing pelB-His₁₀-EcoBamA (Materials and Methods). The residue numbers correspond to *E. coli* BamA unless otherwise stated. To test whether the BamA's last residue W810 is critical for BamA's function, we generated W810F, W810Y, W810V, W810A, W810G and W810D substitutions; the W810F or W810Y substitutions do not slow bacterial growth, while Trp810 substitutions with Val, Ala, Gly or Asp are lethal (Figure 2A). These data suggest that the C-terminal residue of BamA must be aromatic residues. To check whether the BamA variants can be inserted into the OM, the membrane

fraction was collected and western blotting was performed, showing that BamA protein level of the Phe or Tyr substitution in the membrane was similar to those of the wild type BamA. BamA with Gly or Asp substitution was found located in the membrane fraction but the protein level of Val or Ala substitution was extremely low in the membrane (Figure 2B). To further confirm that the BamA variants are inserted into the OM, the urea extraction was performed and BamA variants were detected. As expected, the BamA W810 Phe or Tyr substitution is the same as the wild type in the OM, while BamA mutants W810G and W810D have significantly less than that of the wild type in the OM (Figure 2E). In contrast, no BamA was found in the OM for W810V and W810A mutants (Figure 2E). To check whether the BamA W810V and W810A mutants were degraded by proteinases or could not be inserted into the OM. Whole protein expressions of the Val and Ala substitutions were also examined at mid-logarithmic and late stationary phases, which showed that the protein level of BamA with Val and Ala substitutions were similar at the mid-logarithmic phase to the late stationary phase, but much less than the wild type (Figure 2C, D). These data may suggest that the BamA Val or Ala substitution can be expressed at very low level, but could not be inserted into the OM. The non-inserted BamA variants probably are cleaved by proteases in the periplasm. To further check whether the BamA mutants could be folded properly in the OM, heat modifiability experiments were performed, which showed that W810F, W810Y and W810G are folded properly, while BamA mutants W810D, W810V and W810A were not folded (Figure 2F).

The periplasmic turn 7 is located inside the membrane and is important for function

All the BamA structures suggest that the BamA periplasmic turn 7 is in the OM, based on the Positioning of Proteins in Membrane (PPM) server's prediction (Figure 3A), while the periplasmic turn 7 of another OMP85 family protein TamA (PDB code 4C00), an autotransporter [43], is in the periplasm (Figure 3B), suggesting that BamA periplasmic turn 7 may play an important role for destabilization of the OM. To test this possibility, BamA periplasmic turn 7 variants L780D, L780W and insertion of three Asp residues between P779 and L780 were generated. Hydrophobic tryptophan is well-known for being located inside of the membrane, whereas aspartic acid is a hydrophilic residue that is disfavoured in the membrane. We expected that the L780D mutant and the insertion of the triple Asp residues into the turn 7 would prevent the periplasmic turn 7 from moving inside of the OM, while L780W will help the periplasmic turn to remain in the OM. The functional assays showed that L780D mutant and the triple Asp insertion variant are lethal, but the L780W mutant has no impact on cell growth (Figure 2A). The BamA mutant L780D and the triple Asp insertion variant can be expressed (Figure 2B-D), but the urea extraction experiment indicates that the insertion efficiency was reduced (Figure 2E). It is worth noting that periplasmic turn T7 contains four residues (S778-G781), and deletion of these four residues causes bacteria death (Figure 4A), but it could be expressed and inserted into the OM (Figure 4B). The non-functional deletion BamA may be degraded by the proteinases as the mutant BamA level is similar to the wild-type in the mid-logarithmic phase but much less than the wild-type in the late-logarithmic phase (Figure 2G, H). These data strongly suggest that the periplasmic turn 7 is required to locate inside of the OM for BamA's function.

Periplasmic turns are critical for protein insertion

Our structural work has revealed two conformations of the *E. coli* BAM machinery, indicating that the periplasmic ring rotates around 30° promoting the scissor-like movement of the β 1C- β 6C of BamA barrel with ~65° for unfolded OMP insertion [29]. We observed significant conformational changes of the periplasmic turns between the BamABCDE and BamACDE complexes; particularly, the turns 1 and 2 interact with POTRA 5 and turns 5 and 6 interact with POTRA 3 in BamABCDE complex, while turns 1, 2, 3 and 4 interact with POTRA 5 in BamACDE complex (Figure 3C). We therefore hypothesize that the movement of the barrel strands β 1C- β 6C may mediate through the periplasmic turns. To test this hypothesis, different BamA deletion mutants were generated in periplasmic turns 1, 2, 3, 4, 5, 6 and 7, and functional assays were performed (Figures 3D). The periplasmic turn T1 is formed by ten residues Q446-A455, and a two residue deletion Δ G451-T452 did not affect bacterial growth, while four and six residue deletions of Δ L450-G453 and Δ W449-Y454 resulted in the death of bacteria. T2 contains 10 residues N475-S484, and a four residue deletion Δ T479-G482 has no impact on the bacterial growth, but a full T2 residue deletion Δ N475-S484 is lethal. T3 and T4 contain six residues (P518-N523) and 13 residues (N579-S591), respectively. Interestingly, a four residue deletion Δ N520-N523 of T3 and eight residue deletion Δ D582-D589 of T4 do not impair bacterial growth, suggesting that periplasmic turn T3 and T4 may not play an important role. T5 consists of nine residues (P620-V628). Two residue deletion Δ D623-D624 of turn T5 did not slow bacterial growth. In contrast, both four residue deletion Δ D622-H625 and nine residue deletion Δ P620-V628 of turn T5 kill the bacteria. The western blot showed that the level of the BamA deletions Δ D622-H625 and Δ P620-V628 significantly lower in the late-logarithmic phase than that of the mid-logarithmic phase, indicating that the BamA two deletions are degraded by the

proteinases. T6 has 14 residues (T720-V733). Four residue deletion Δ S726-Y729 of turn T6 has no affection on bacterial growth, while 14 residue deletion Δ T720-V733 is lethal. Similar to the turn T5 deletions Δ D622-H625 and Δ P620-V628, the BamA T6 turn Δ T720-V733 deletion was degraded (Figure 2G, H). These data may suggest that periplasmic turn deletions could express to the similar level of the wild-type, but the lethal mutants are degraded by the outer membrane protein quality control proteinases.

Extracellular loops play a less important role in OMP insertion

BamA barrel β 1C- β 6C has scissor-like movement; the extracellular loops 1-3 have significant conformational changes between BamABCDE and BamACDE complexes, from pointing to the barrel to the outer side of the bacteria (Figure S5). BamA deletion mutants were generated in extracellular loops 1, 2 and 3, and functional assays were performed (Figure 4A). L1 consists of four residues G433-S436 and L1 four residue deletion Δ T434-G437 does not impair bacteria growth, but deletion of Y432-V438 including residues of β 1C and β 2C causes bacterial death. L2 contains five residues K462-Q466; deletion of four residues Δ N463-Q466 slows the bacteria growth. L3 consists of 11 residues Q495-T505; deletion of four residues Δ A499-S502 do not show a growth defect, but delete the whole loop impairs cell growth. All BamA variants with loop deletions are expressed into the membrane fraction (Figure 5B). These data suggest that the extracellular loops 1-3 play less important or no role for OM insertion.

Discussion

In Gram-negative bacteria, outer membrane barrel proteins are inserted and folded into the OM by BAM machinery. Our structural and functional studies of the BAM machinery suggest that the BAM machinery inserts OMP into the OM by periplasmic ring rotation that promotes the barrel conformational changes to insert OMPs without using ATP [29]. The SSM analysis showed that the BamA barrel structure of *S. enterica* is similar to those of *E. coli* (PDB code 5D0O [29]; PDB code 4C4V [17]) and *N. gonorrhoeae* (PDB code 4K3B [14]) with RMSD of 1.84 Å over 290 aligned residues, 1.73 Å over 288 aligned residues, and 2.418 Å over 249 aligned residues, respectively. In particular, these four barrels share the similar structural feature that all the C-termini of β 16C coil into the lumen of the barrel. This may be involved in “thinning” the OM and disturbing the OM for outer membrane protein insertion [14].

Bacterial OMP β -signature sequence is important for OMP insertion and the β -signature sequences are at the C-terminal residues for most of the β -barrel protein with the last residue is normally Phe or Trp. More recently, the β -signature sequence of BamA is reported to be N765-P779, which forms the β 14C and binds to BamD [42]. The *Salmonella* BamA structure showed that the C-terminal residues shift to the lumen, which is similar to those of the BamA structure from *E. coli*, and BamA C-terminus is Trp. *E. coli* BamA W810 substitutions revealed that the aromatic residue substitutions are functional, but other mutants are lethal. The BamA could not be inserted into the OM if Trp810 is mutated into the non-aromatic hydrophobic residues Val or Ala, even though the protein can be expressed. In contrast, BamA variants W810G or W810D can be inserted into the OM, but they are not functional. These data suggest that the aromatic residue Trp810 is not only for BamA insertion, but also for BamA's function for destabilizing OM, probably through movement inside the OM. Addition of four Asp residues after W810 prevents the Trp810 movement in the

OM and kills the bacteria, which further confirmed this notion. The lipid heads of the inner leaflet of the OM prevent unfolded OMP insertion into the OM [44] and OM destabilization is required for the OMP insertion. The periplasmic turn deletion assays revealed that partial deletion of the turns T1, T2 and T5 kill the bacteria, while the whole turn T6 deletion causes the death of the bacteria. In contrast, deletions of T3 and T4 have no effect on bacterial growth. These data are consistent with the structural findings. In the BamABCDE complex T1 and T2 interact with POTRA5 while T5 and T6 interact with POTRA3; in this instance the dimension of the central hole of periplasmic ring is around 46 Å x 20Å. However, the T1, T2, T3 and T4 interact with the POTRA5, with the T3 and T4 having fewer contacts with POTRA5 than T1 and T2, while T5 and T6 do not interact with POTRA3 in BamACDE complex making the dimension of the central hole of the ring about 34 Å x 33Å. At the same time the β 1C- β 6C adopt the significant conformational changes. These data may strongly suggest that the periplasmic turns T1, T2, T5 and T6 may play an important role in mediating the periplasmic ring rotation to the barrel strands β 1C- β 6C's movement. In addition, periplasmic turn 7 is located within the membrane, which may play a role in destabilising the OM and helping OMP insertion.

The whole L1 deletion Δ T434-G437 shows no bacterial growth defect. Although deletion Δ Y432-V438 causes bacterial death, this deletion not only deletes L1 loop residues, but also deletes residues of β 1C and β 2C. Deletion of individual loop 2 or 3 has some or no impact for bacterial growth. These data suggest that the extracellular loops 1-3 may play less important role in OMP insertion than those of the periplasmic turns, but play a role in sequestering the intact barrel from the environment.

Abbreviations

Ala, Alanine; Asp, Aspartate; ATP, adenosine triphosphate; BAM, β -barrel assembly machinery; Gly, Glycine; IM, inner membrane; IPTG, isopropyl β -d-1-thiogalactopyranoside; LDAO, n-Dodecyl-N,N-Dimethylamine-N-Oxide; Ni-NTA, nickel-nitrilotriacetic acid; OEP80; outer envelope protein of 80 kDa; OG, n-Octyl- β -D-Glucopyranoside; OM, outer membrane; OMP85, outer membrane protein of 85 kDa; OMPs, outer membrane proteins; PDB, protein data bank; Phe, Phenylalanine; POTRA, polypeptide transport associated; p.s.i, pounds per square inch; PVDF, polyvinylidene difluoride; RMSD, root-mean-square deviation; SAM50, Sorting assembly machinery 50 kDa subunit; SB3-14, 3-(N,N-Dimethylmyristylammonio)propanesulfonate; SSM, secondary-structure matching; TBS, tris-buffered saline; Trp, tryptophan; Tyr, Tyrosine; Val, Valine.

Authors contributions

C.D. conceived and supervised the project; Y.G., Y.Z. and Z.W. performed the experiments and analyzed data; C.D. and Y.G. solved the structure and wrote the manuscript.

Funding

C.D. is a recipient of the Wellcome Trust investigator award [WT106121MA] and is supported by Medical Research Council [G1100110/1].

Acknowledgements

We thank Prof. Thomas J. Silhavy for providing JCM166 cells. We thank Diamond Light Source for access to beamtime i04-1 (proposal mx9475) that contributed to the results presented here.

Competing interests

The Authors declare that there are no competing interests associated with the manuscript.

Availability of supporting data

BamA coordinate and structure factor of *S. Typhimurium* have been deposited in Protein Data Bank under access code 5OR1.

Appendix A. Supplementary Data

References

1. Knowles, T. J., Scott-Tucker, A., Overduin, M. and Henderson, I. R. (2009) Membrane protein architects: the role of the BAM complex in outer membrane protein assembly. *Nat. Rev. Microbiol.* **7**, 206-214 doi: 10.1038/nrmicro2069
2. Walther, D. M., Rapaport, D. and Tommassen, J. (2009) Biogenesis of beta-barrel membrane proteins in bacteria and eukaryotes: evolutionary conservation and divergence. *Cell Mol. Life Sci.* **66**, 2789-2804 doi: 10.1007/s00018-009-0029-z
3. Arnold, T., Zeth, K. and Linke, D. (2010) Omp85 from the thermophilic cyanobacterium *Thermosynechococcus elongatus* differs from proteobacterial Omp85 in structure and domain composition. *J. Biol. Chem.* **285**, 18003-18015 doi: 10.1074/jbc.M110.112516
4. Koenig, P., Mirus, O., Haarmann, R., Sommer, M. S., Sinning, I., Schleiff, E. and Tews, I. (2010) Conserved properties of polypeptide transport-associated

- (POTRA) domains derived from cyanobacterial Omp85. *J. Biol. Chem.* **285**, 18016-18024 doi: 10.1074/jbc.M110.112649
5. Wu, T., Malinverni, J., Ruiz, N., Kim, S., Silhavy, T.J. and Kahne, D. (2005) Identification of a multicomponent complex required for outer membrane biogenesis in *Escherichia coli*. *Cell*.**121**, 235-245 doi: 10.1016/j.cell.2005.02.015
 6. Heinz, E. and Lithgow, T. (2014) A comprehensive analysis of the Omp85/TpsB protein superfamily structural diversity, taxonomic occurrence, and evolution. *Front. Microbiol.* **5**, 370 doi: 10.3389/fmicb.2014.00370
 7. Kim, S., Malinverni, J. C., Sliz, P., Silhavy, T. J., Harrison, S. C. and Kahne, D. (2007) Structure and function of an essential component of the outer membrane protein assembly machine. *Science*. **317**, 961-964 doi: 10.1126/science.1143993
 8. Tommassen, J. (2010) Assembly of outer-membrane proteins in bacteria and mitochondria. *Microbiology*. **156**, 2587-2596 doi: 10.1099/mic.0.042689-0
 9. Webb, C. T., Heinz, E. and Lithgow, T. (2010) Evolution of the beta-barrel assembly machinery. *Trends Microbiol.* **20**, 612-620 doi: 10.1016/j.tim.2012.08.006
 10. Day, P. M., Potter, D. and Inoue, K. (2014) Evolution and targeting of Omp85 homologs in the chloroplast outer envelope membrane. *Front. Plant Sci.* **5**, 535 doi: 10.3389/fpls.2014.00535
 11. Rigel, N. W. and Silhavy, T. J. (2012) Making a beta-barrel: assembly of outer membrane proteins in Gram-negative bacteria. *Curr. Opin. Microbiol.***15**, 189-193 doi: 10.1016/j.mib.2011.12.007
 12. Rossiter, A. E., Leyton, D. L., Tveen-Jensen, K., Browning, D. F., Sevastyanovich, Y., Knowles, T. J., Nichols, K. B., Cunningham, A. F., Overduin, M., Schembri, M. A. and Henderson, I. R. (2011) The essential beta-barrel

assembly machinery complex components BamD and BamA are required for autotransporter biogenesis. *J. bacteriol.* **193**, 4250-4253 doi: 10.1128/JB.00192-11

13. Noinaj, N., Fairman, J. W. and Buchanan, S. K. (2011) The Crystal Structure of BamB Suggests Interactions with BamA and Its Role within the BAM Complex. *J. Mol. Biol.* **407**, 248-260 doi: 10.1016/j.jmb.2011.01.042
14. Noinaj, N., Kuszak, A. J., Gumbart, J. C., Lukacik, P., Chang, H., Easley, N. C., Lithgow, T. and Buchanan, S. K. (2013) Structural insight into the biogenesis of beta-barrel membrane proteins. *Nature.* **501**, 385-390 doi: 10.1038/nature12521
15. Zhang, H., Gao, Z. Q., Hou, H. F., Xu, J. H., Li, L. F., Su, X. D. and Dong, Y. H. (2011) High-resolution structure of a new crystal form of BamA POTRA4-5 from *Escherichia coli*. *Acta Crystallogr. Sect. F Struct. Biol. Cryst. Commun.* **67**, 734-738 doi: 10.1107/S1744309111014254
16. Ni, D., Wang, Y., Yang, X., Zhou, H., Hou, X., Cao, B., Lu, Z., Zhao, X., Yang, K. and Huang, Y. (2014) Structural and functional analysis of the beta-barrel domain of BamA from *Escherichia coli*. *FASEB J.* **28**, 2677-2685 doi: 10.1096/fj.13-248450
17. Albrecht, R., Schutz, M., Oberhettinger, P., Faulstich, M., Bermejo, I., Rudel, T., Diederichs, K. and Zeth, K. (2014) Structure of BamA, an essential factor in outer membrane protein biogenesis. *Acta Crystallogr. D Biol. Crystallogr.* **70**, 1779-1789 doi: 10.1107/S1399004714007482
18. Albrecht, R. and Zeth, K. (2011) Structural basis of outer membrane protein biogenesis in bacteria. *J. Biol. Chem.* **286**, 27792-27803 doi: 10.1074/jbc.M111.238931

19. Kim, K. H. and Paetzel, M. (2011) Crystal structure of *Escherichia coli* BamB, a lipoprotein component of the beta-barrel assembly machinery complex. *J. Mol. Biol.* **406**, 667-678 doi: 10.1016/j.jmb.2010.12.020
20. Kim, K. H., Aulakh, S. and Paetzel, M. (2011) Crystal structure of beta-barrel assembly machinery BamCD protein complex. *J. Biol. Chem.* **286**, 39116-39121 doi: 10.1074/jbc.M111.298166
21. Kim, K. H., Aulakh, S., Tan, W. and Paetzel, M. (2011) Crystallographic analysis of the C-terminal domain of the *Escherichia coli* lipoprotein BamC. *Acta Crystallogr. Sect. F Struct. Biol. Cryst. Commun.* **67**, 1350-1358 doi: 10.1107/S174430911103363X
22. Kim, K. H., Kang, H. S., Okon, M., Escobar-Cabrera, E., McIntosh, L. P. and Paetzel, M. (2011) Structural characterization of *Escherichia coli* BamE, a lipoprotein component of the beta-barrel assembly machinery complex. *Biochemistry.* **50**, 1081-1090 doi: 10.1021/bi101659u
23. Warner, L. R., Varga, K., Lange, O. F., Baker, S. L., Baker, D., Sousa, M. C. and Pardi, A. (2011) Structure of the BamC two-domain protein obtained by Rosetta with a limited NMR data set. *J. Mol. Biol.* **411**, 83-95 doi: 10.1016/j.jmb.2011.05.022
24. Knowles, T. J., Browning, D. F., Jeeves, M., Maderbocus, R., Rajesh, S., Sridhar, P., Manoli, E., Emery, D., Sommer, U., Spencer, A., Leyton, D. L., Squire, D., Chaudhuri, R. R., Viant, M. R., Cunningham, A. F., Henderson, I. R. and Overduin, M. (2011) Structure and function of BamE within the outer membrane and the beta-barrel assembly machine. *EMBO Rep.* **12**, 123-128 doi: 10.1038/embor.2010.202

25. Sandoval, C. M., Baker, S. L., Jansen, K., Metzner, S. I. and Sousa, M. C. (2011) Crystal Structure of BamD: An Essential Component of the beta-Barrel Assembly Machinery of Gram-Negative Bacteria. *J. Mol. Biol.* **409**, 348-357 doi: 10.1016/j.jmb.2011.03.035
26. Dong, C., Hou, H. F., Yang, X., Shen, Y. Q. and Dong, Y. H. (2012) Structure of *Escherichia coli* BamD and its functional implications in outer membrane protein assembly. *Acta Crystallogr. D Biol. Crystallogr.* **68**, 95-101 doi: 10.1107/S0907444911051031
27. Jansen, K. B., Baker, S. L. and Sousa, M. C. (2015) Crystal Structure of BamB Bound to a Periplasmic Domain Fragment of BamA, the Central Component of the beta-Barrel Assembly Machine. *J. Biol. Chem.* **290**, 2126-36 doi: 10.1074/jbc.M114.584524
28. Bergal, H. T., Hopkins, A. H., Metzner, S. I. and Sousa, M. C. (2016) The Structure of a BamA-BamD Fusion Illuminates the Architecture of the beta-Barrel Assembly Machine Core. *Structure.* **24**, 243-251 doi: 10.1016/j.str.2015.10.030
29. Gu, Y., Li, H., Dong, H., Zeng, Y., Zhang, Z., Paterson, N. G., Stansfeld, P. J., Wang, Z., Zhang, Y., Wang, W. and Dong, C. (2016) Structural basis of outer membrane protein insertion by the BAM complex. *Nature.* **531**, 64-69 doi: 10.1038/nature17199
30. Bakelar, J., Buchanan, S. K. and Noinaj, N. (2016) The structure of the beta-barrel assembly machinery complex. *Science.* **351**, 180-186 doi: 10.1126/science.aad3460
31. Han, L., Zheng, J., Wang, Y., Yang, X., Liu, Y., Sun, C., Cao, B., Zhou, H., Ni, D., Lou, J., Zhao, Y. and Huang, Y. (2016) Structure of the BAM complex and its

- implications for biogenesis of outer-membrane proteins. *Nat. Struct. Mol. Biol.* **23**, 192-196 doi: 10.1038/nsmb.3181
32. Iadanza, M.G., Higgins, A.J., Schiffrin, B., Calabrese, A.N., Brockwell, D.J., Ashcroft, A.E., Radford, S.E. and Ranson, N.A. (2016) Lateral opening in the intact beta-barrel assembly machinery captured by cryo-EM, *Nat. Commun.* **7**, 12865 doi: 10.1038/ncomms12865
33. Fardini, Y., Trotereau, J., Bottreau, E., Souchard, C., Velge, P. and Virlogeux-Payant, I. (2009) Investigation of the role of the BAM complex and SurA chaperone in outer-membrane protein biogenesis and type III secretion system expression in *Salmonella*. *Microbiology*. **155**, 1613-1622 doi: 10.1099/mic.0.025155-0
34. Liu, H. and Naismith, J. H. (2008) An efficient one-step site-directed deletion, insertion, single and multiple-site plasmid mutagenesis protocol. *BMC Biotechnol.* **8**, 91 doi: 10.1186/1472-6750-8-91
35. Winn, M. D., Ballard, C. C., Cowtan, K. D., Dodson, E. J., Emsley, P., Evans, P. R., Keegan, R. M., Krissinel, E. B., Leslie, A. G., McCoy, A., McNicholas, S. J., Murshudov, G. N., Pannu, N. S., Potterton, E. A., Powell, H. R., Read, R. J., Vagin, A. and Wilson, K. S. (2011) Overview of the CCP4 suite and current developments. *Acta Crystallogr. D Biol. Crystallogr.* **67**, 235-242 doi: 10.1107/S0907444910045749
36. McCoy, A. J., Grosse-Kunstleve, R. W., Adams, P. D., Winn, M. D., Storoni, L. C. and Read, R. J. (2007) Phaser crystallographic software. *J. Appl. Crystallogr.* **40**, 658-674 doi: 10.1107/S0021889807021206

37. Emsley P. and Cowtan, K. (2004) Coot: model-building tools for molecular graphics. *Acta Crystallogr. D Biol. Crystallogr.* **60**:2126-2132 doi: 10.1107/S0907444904019158
38. Murshudov, G. N., Vagin, A. A. and Dodson, E. J. (1997) Refinement of macromolecular structures by the maximum-likelihood method. *Acta Crystallogr. D Biol. Crystallogr.* **53**, 240-255 doi: 10.1107/S0907444996012255
39. Leo, J. C., Oberhettinger, P. and Linke, D. (2015) Assessing the Outer Membrane Insertion and Folding of Multimeric Transmembrane beta-Barrel Proteins. *Methods Mol. Biol.* **1329**, 157-167 doi: 10.1007/978-1-4939-2871-2_12
40. Krissinel, E. and Henrick, K. (2004) Secondary-structure matching (SSM), a new tool for fast protein structure alignment in three dimensions. *Acta Crystallogr. D Biol. Crystallogr.* **60**, 2256-2268 doi: 10.1107/S0907444904026460
41. Lehr, U., Schutz, M., Oberhettinger, P., Ruiz-Perez, F., Donald, J. W., Palmer, T., Linke, D., Henderson, I. R. and Autenrieth, I. B. (2010) C-terminal amino acid residues of the trimeric autotransporter adhesin YadA of *Yersinia enterocolitica* are decisive for its recognition and assembly by BamA. *Mol. Microbiol.* **78**, 932-946 doi: 10.1111/j.1365-2958.2010.07377.x
42. Hagan, C. L., Wzorek, J. S. and Kahne, D. (2015) Inhibition of the beta-barrel assembly machine by a peptide that binds BamD. *Proc. Natl Acad. Sci. U.S.A.* **112**, 2011-2016 doi: 10.1073/pnas.1415955112
43. Gruss, F., Zahringer, F., Jakob, R. P., Burmann, B. M., Hiller, S. and Maier, T. (2013) The structural basis of autotransporter translocation by TamA. *Nat. Struct. Mol. Biol.* **20**, 1318-1320 doi: 10.1038/nsmb.2689
44. Gessmann, D., Chung, Y. H., Danoff, E. J., Plummer, A. M., Sandlin, C. W., Zaccai, N. R. and Fleming, K. G. (2014) Outer membrane beta-barrel protein

folding is physically controlled by periplasmic lipid head groups and BamA. *Proc. Natl Acad. Sci. U.S.A.* **111**, 5878-5883 doi: 10.1073/pnas.1322473111

Table 1. Data collection and refinement statistics

Data collection	BamA
Space group	P6 ₂ 2 2
Cell dimensions	
a, b, c (Å)	124.03, 124.03, 131.48
α , β , γ (°)	90.0, 90.0, 120.0
Wavelength (Å)	0.9200
Resolution (Å)	130-2.92 (3.024 - 2.92)
I / σ	7.7(2.5)
Unique reflections	13411(1311)
Completeness	100% (100%)
Redundancy	17.3(18.2)
R _{merge}	0.30/1.52

CC1/2	0.99(0.5)
Refinement	
Resolution (Å)	130-2.92 (3.02-2.92)
R _{work} (%)	0.28(0.43)
R _{free} (%)	0.34(0.5)
RMS(bonds)	0.012
RMS(angles)	1.8
Ramachandran favored (%)	91
Ramachandran allowed (%)	6
PDB access code	5OR1

Figure legends

Figure 1 | Structure of SenBamA β barrel. (A) SDS-PAGE analysis of purified SenBamAB protein complex. (B) Crystal structure of SenBamA β barrel. Cartoon representation of SenBamA β barrel in rainbow. The side view and the top view of the SenBamA. (C) The structure of SenBamA is similar to EcoBamA barrel. SenBamA in rainbow is superimposed well with EcoBamA (PDB code 5D0O) in magenta.

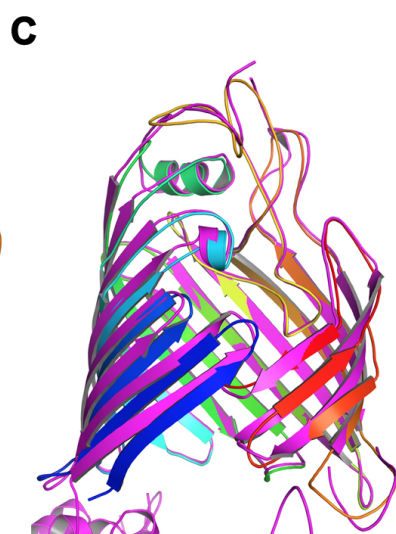
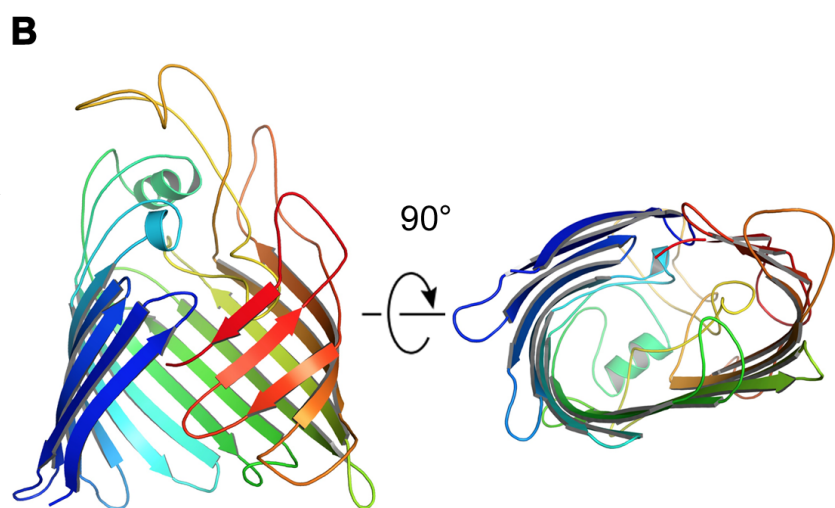
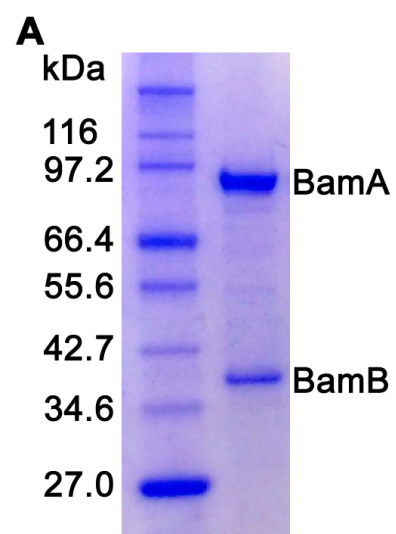
Figure 2 | C-terminal strand β 16C terminal residue and periplasmic turn 7 are critical for BamA functionality. (A) Functional assays of BamA variants of the C-terminal strand and periplasmic turn 7. Numbers 1 – 13 represent BamA depleted strain JCM166 harboring wild-type BamA, empty vector, BamA variants W810F,

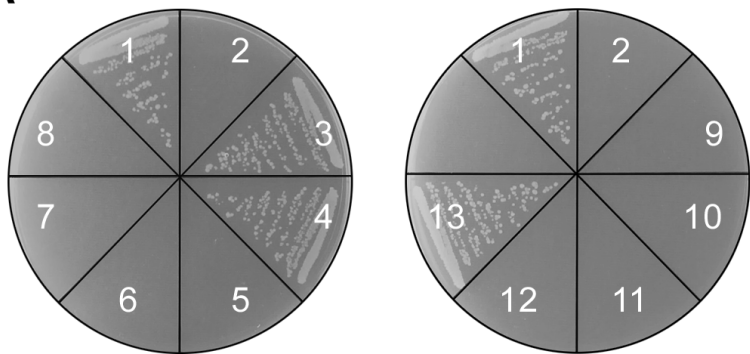
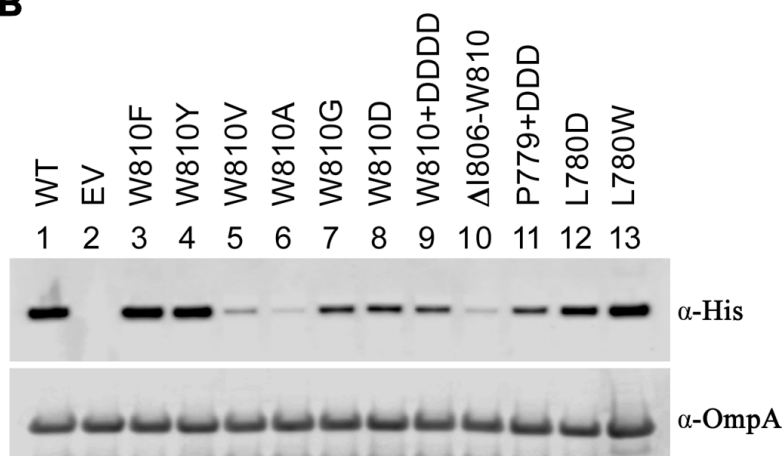
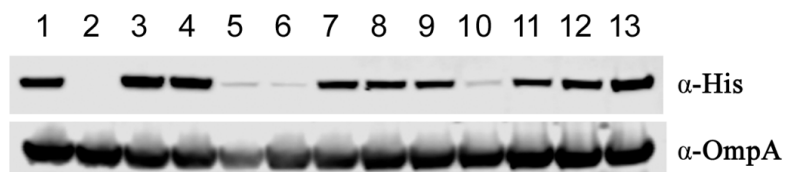
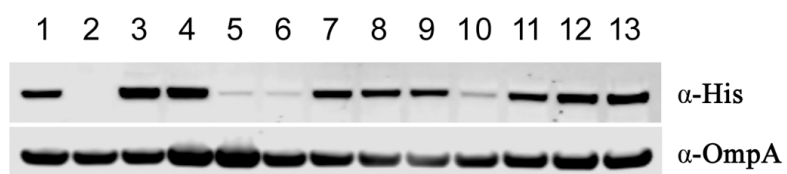
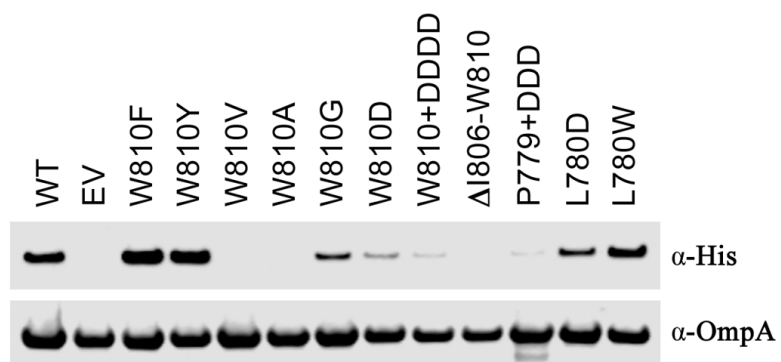
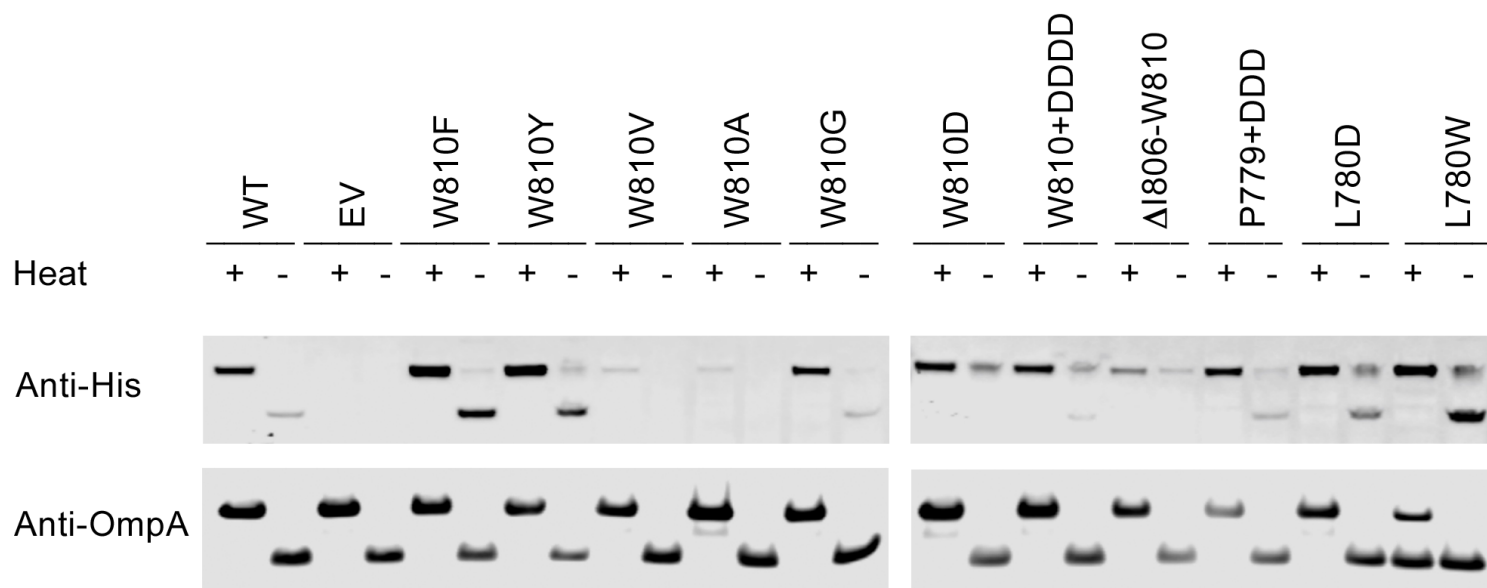
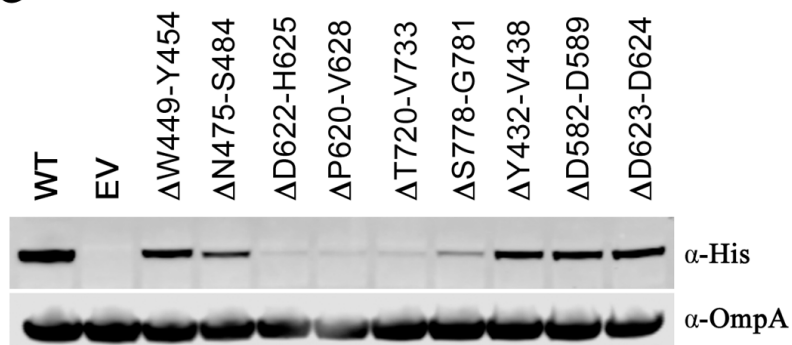
W810Y, W810V, W810A, W810G, W810D, W810+DDDD, Δ I810-W810, P779+DDD, L780D and L780W, respectively. (B) Western Blot analysis of protein expression levels of wild-type BamA and its variants in the cell membrane. (C) Western Blot analysis of protein expression levels of wild-type BamA and its variants with total cell lysate of cells in late stationary phase. (D) Western Blot analysis of protein expression levels of wild-type BamA and its variants with total cell lysate of cells in mid-logarithmic phase. (E) Urea extraction analysis of protein expression levels of wild-type BamA and its variants. (F) Heat modifiability analysis of protein expression levels of wild-type BamA and its variants. (G) Western Blot analysis of protein expression levels of wild-type BamA and its variants with total cell lysate of cells in late stationary phase. (H) Western Blot analysis of protein expression levels of wild-type BamA and its variants with total cell lysate of cells in mid-logarithmic phase.

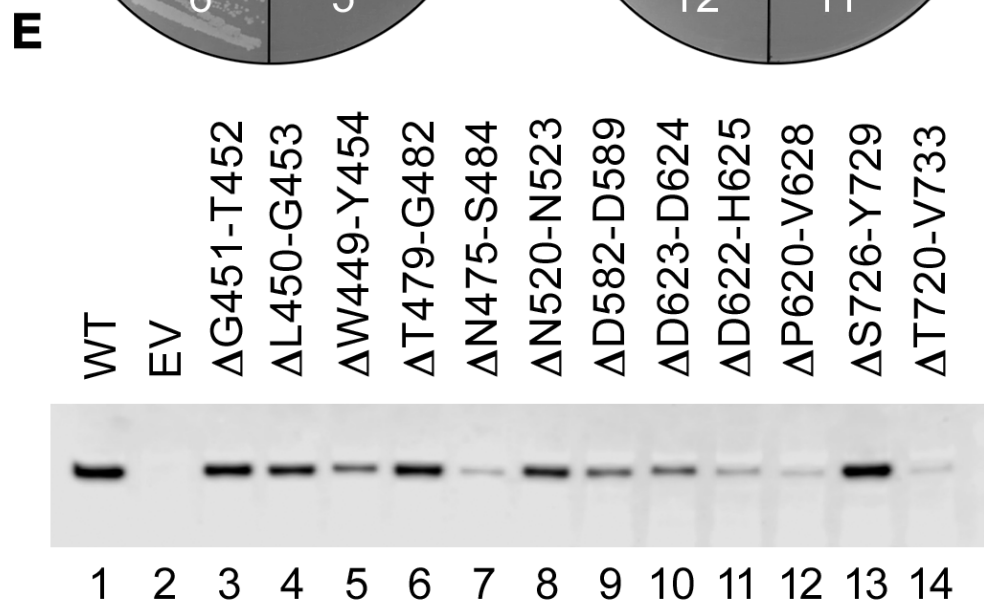
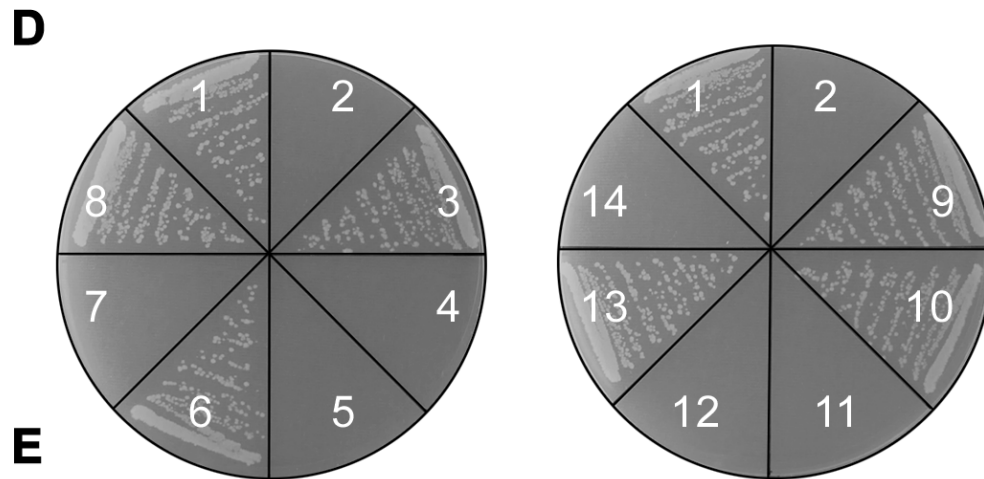
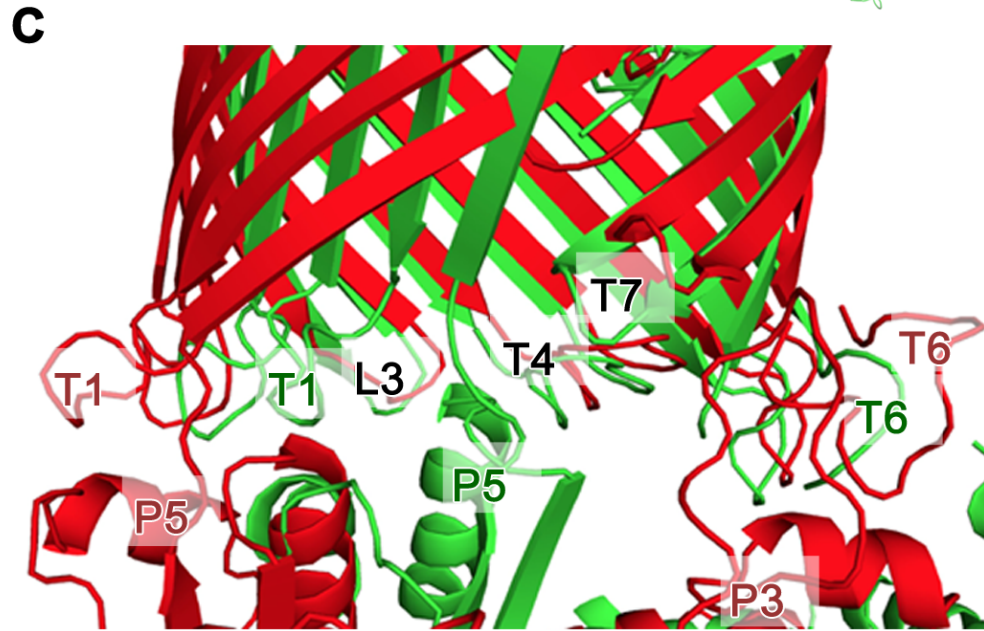
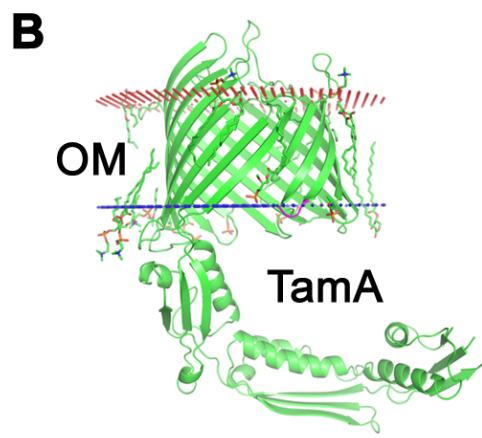
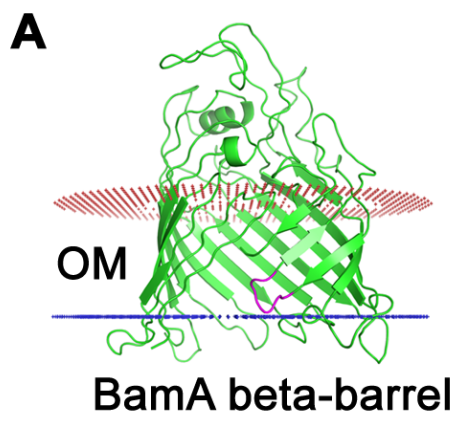
Figure 3 | Periplasmic turns are important for the BamA's function. (A) The PPM server predicts that the periplasmic turn 7 of EcoBamA in the OM. (B) The PPM server predicts that the periplasmic turn 7 of TamA in the periplasm. (C) The periplasmic turns adopt significant conformational changes from structure BamABCDE in red to BamACDE in green. (D) Functional assays of the periplasmic turn deletions. Numbers 1 – 14 represent BamA depleted strain JCM166 harboring wild-type BamA, empty vector, BamA mutations Δ G451-T452, Δ L450-G453, Δ W449-Y454, Δ T479-G482, Δ N475-S484, Δ N520-N523, Δ D582-D589, Δ D623-D624, Δ D622-H625, Δ P620-V628, Δ S726-Y729 and Δ T720-V733, respectively. (E) Western Blot analysis of protein expression levels of wild-type BamA and its variants in the cell membrane.

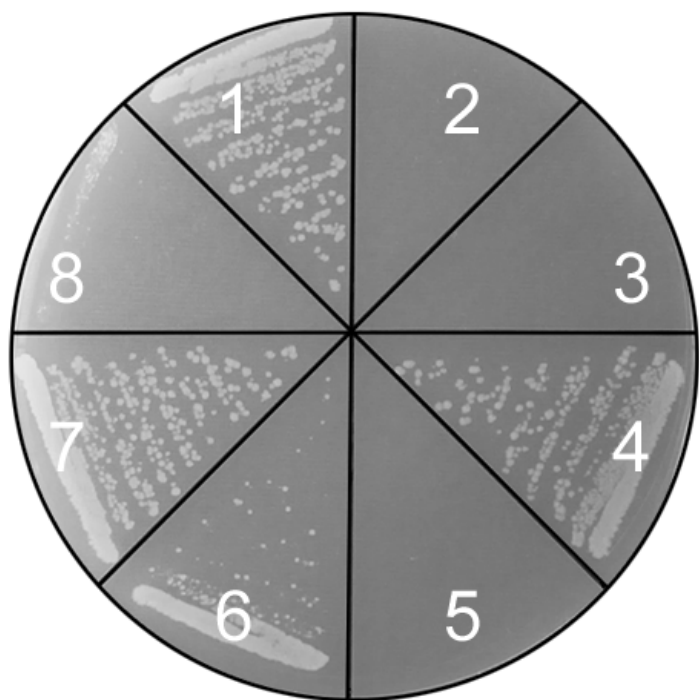
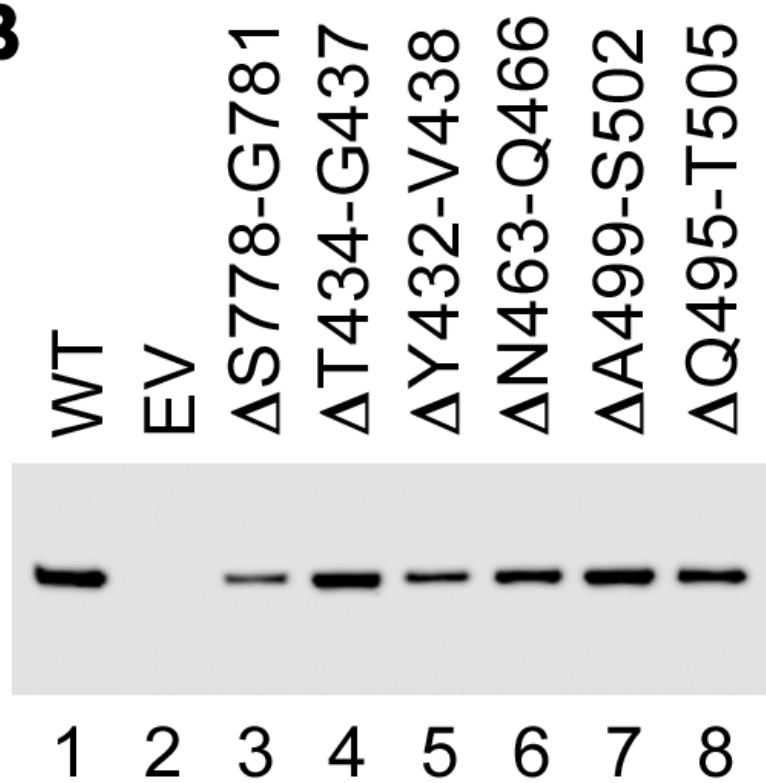
Figure 4 | Extracellular loops 1-3 play less important role in OMP insertion. (A)

Functional assays of BamA periplasmic turn 7 deletion and extracellular loop deletions. Numbers 1 – 8 represent BamA depleted strain JCM166 harboring wild-type BamA, empty vector, BamA mutations Δ S778-G781, Δ T434-G437, Δ Y432-V438, Δ N463-Q466, Δ A499-S502 and Δ Q495-T505, respectively. (B) Western Blot analysis of protein expression levels of wild-type BamA and its variants in the cell membrane.



A**B****C****D****E****F****G****H**



A**B**

Supplementary information

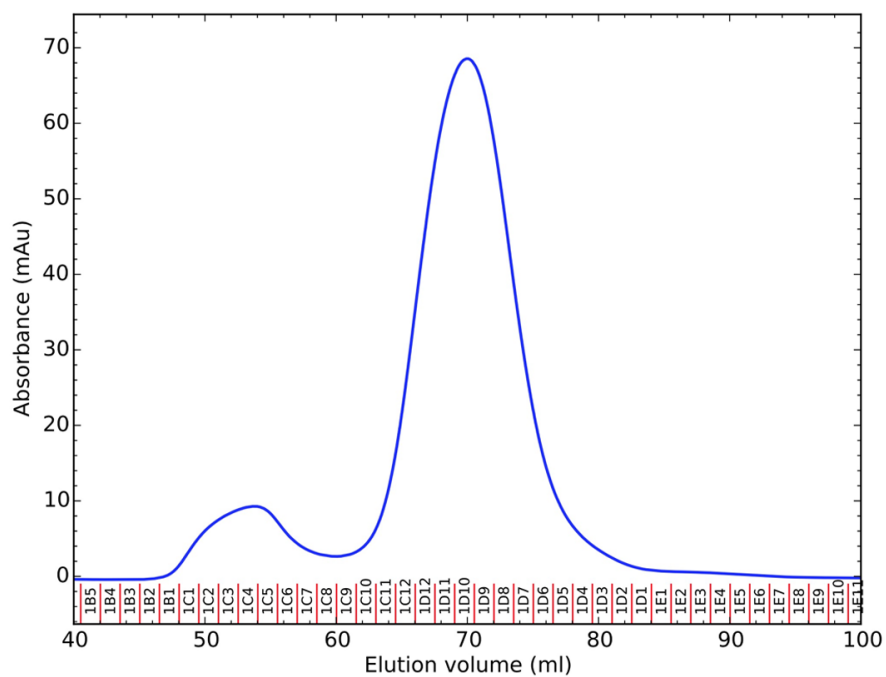


Figure S1. The gel filtration of the BamA-BamB complex. The gel filtration was performed at 1ml/min using HiLoad 16/600 Superdex 200pg. The peak fraction (at 70ml) was collected and the sample was analysed by SDS-PAGE with Coomassie staining (Figure 1), showing the BamA-BamB complex.

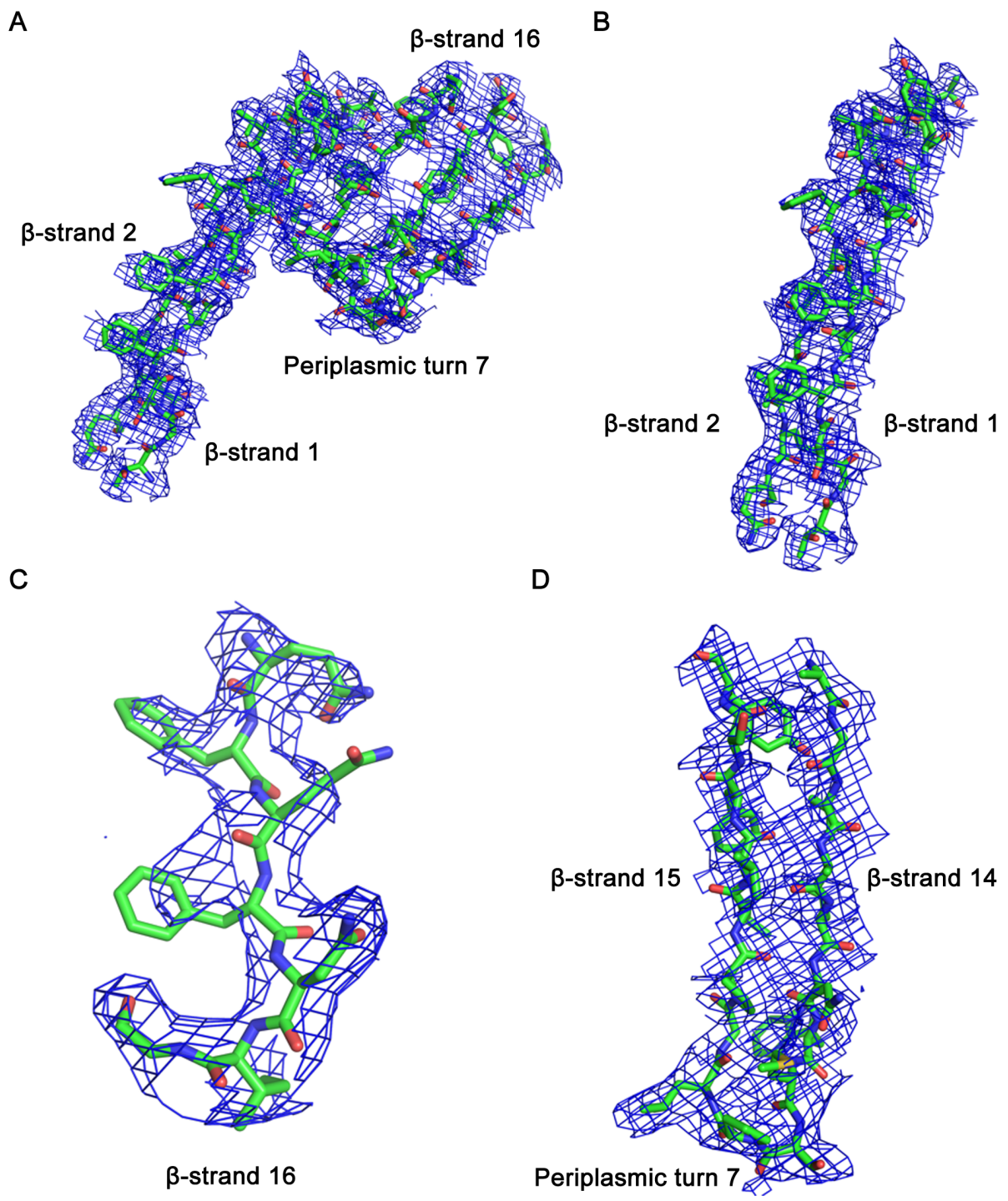


Figure S2. 2Fo-Fc electron density map of the BamA contoured at 1σ .



Figure S3. The β 16C coils into the barrel. Superimposition of BamA barrel domains of *Salmonella enterica* in red with *E. coli* BamA barrels of BamABCDE in magenta and BamACDE in green. The β 16C of BamACDE complex moves the deepest inside of the barrel.

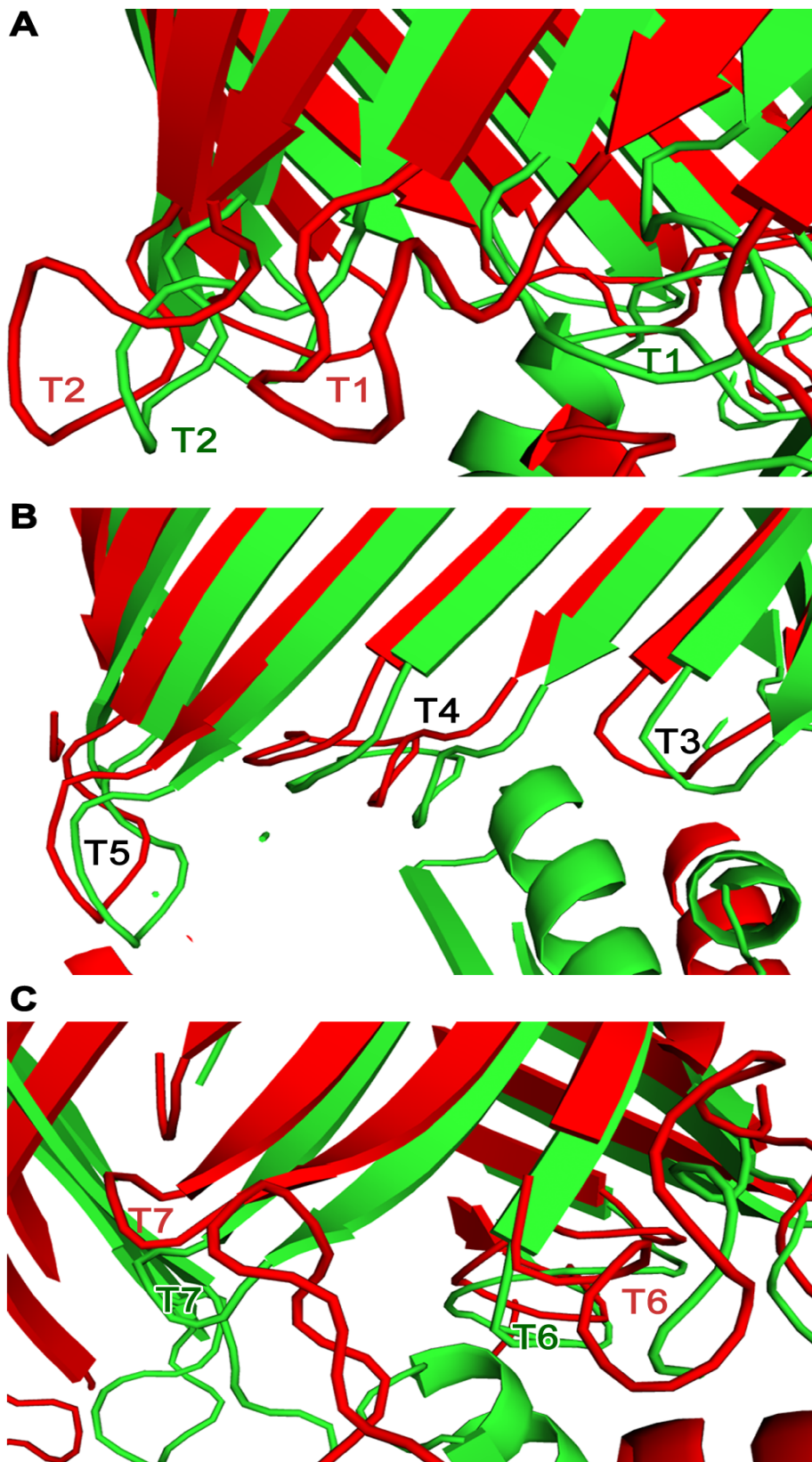


Figure S4. The conformational changes of the periplasmic turns from BamABCDE to BamACDE complex. The BamABCDE complex in red, and BamACDE complex in green. (A), Periplasmic turn 1 and 2. (B), Periplasmic turn 3, 4 and 5. (C), Periplasmic turn 6 and 7.

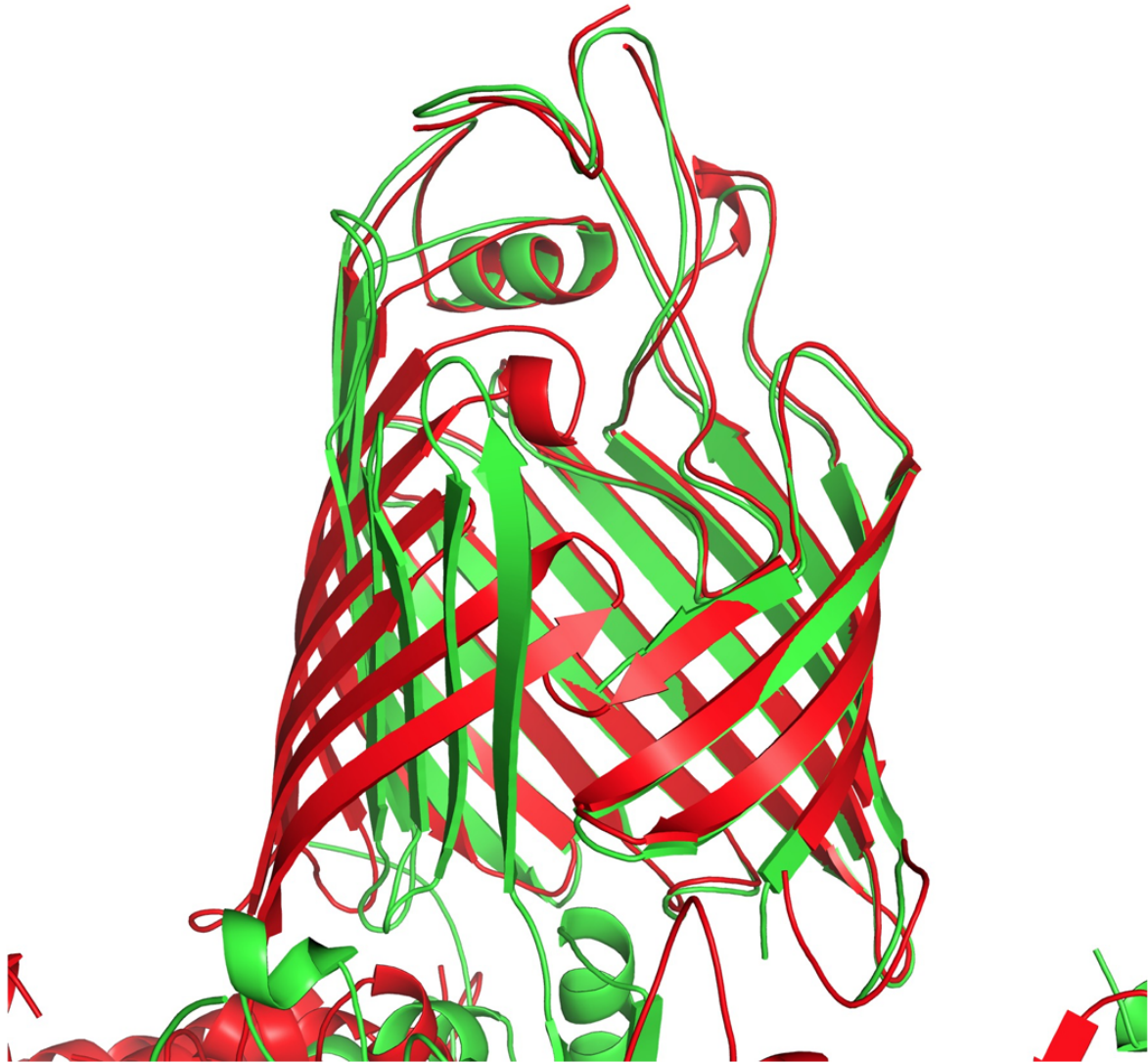


Figure S5. The conformational changes of the extracellular loops 1, 2 and 3. The BamA of BamABCDE in red and BamA of BamACDE in green. The extracellular loops 1, 2 and 3 are pointing to the pore in BamABCDE, helping to seal the pore, while the extracellular loops 1, 2 and 3 are pointing out of the bacteria in BamACDE complex.